

Toward 10-Milliarcsecond Infrared Astrometry

Robert N. Treuhaft

Stephen I'. Lowe

Jet Propulsion Laboratory
Pasadena, California 91109

Manfred Bester

William C. Danchi

Charles H. Townes

Space Sciences Laboratory
University of California at Berkeley
Berkeley, California 94720

ABSTRACT

Infrared astrometry at the 10-milliarcsecond (mas) level is applicable to experiments in stellar evolution astronomy, solar system dynamics, relativistic gravitation, and deep space laser tracking. We are pursuing astrometry with the U. C. Berkeley Infrared Spatial Interferometer (ISI) on Mt. Wilson to demonstrate a 10-mas capability for tracking stellar and solar system objects. Astrometric data from the ISI, taken and analyzed over the last 5 years, have shown that instrumental and atmospheric effects limit current demonstrations. The ISI data show that point-to-point interferometric phase fluctuations due to tropospheric and quantum noise, for optimal integration times of 0.2 seconds, are approaching the 0.1 -cycle level needed to reliably connect the phase. Modeling the ISI data suggests that atmospheric fluctuations on Mt. Wilson, during the best seeing, are dominated by a low-lying component, within the first 25 meters above the ISI, which, in the future, may be minimized with *in situ* calibration. A calculation of atmosphere-limited astrometric accuracy shows that the ISI will soon be able to achieve 10-mas astrometry, on a 13-m baseline in a single observing session, employing current ground-based laser distance interferometer calibrations to minimize atmospheric effects.

1. INTRODUCTION

This paper describes the instrumental and atmospheric limitations of ISI infrared astrometry, and a proposed route to achieving 10-mas astrometric accuracy. As will be shown in section 2, instrumental system noise limitations make interferometric phase connection possible only for observations with good seeing. While instrumental error contributions will be reduced over the next few years, atmospheric refractivity fluctuations studied with the ISI are likely to be the dominant astrometric errors for all galactic and solar system targets. Section 3 describes a model calculation of the Mt. Wilson atmospheric turbulence height profile, and calculates limiting atmospheric astrometric errors. Modeling the correlation between path length fluctuations in the telescopes and atmosphere suggests that the dominant contribution from the turbulent atmosphere originates only a few tens of meters above the ISI, on nights of good seeing. This description of the Mt. Wilson atmospheric behavior may well apply to other mountain-top astronomical sites. Section 4 describes the potential for up-

grading both the instrumentation and analysis algorithms to achieve astrometry at the 10-mas level, which would be almost an order of magnitude better than previous infrared astrometric results¹.

2. INSTRUMENTAL LIMITATIONS

This section describes the instrumental limitations to current IS1 astrometric demonstrations, with emphasis on system noise limitations. Each of the two telescopes of the IS1 consists of a steerable flat mirror, a focusing parabolic mirror, and heterodyne electronics which convert the infrared signal to a 2-GHz wide radio signal for cross correlation.² Helium-neon laser distance interferometers (HeNe LDIs) in each telescope monitor the path lengths between the flat and parabolic mirrors and behind the flat mirror to the optics table. The sensitivity of the IS1 for infrared astrometry is limited by the noise in the output of the heterodyne receivers, which is about twice the quantum limit, or equivalent to about 2600 °K single-sideband system temperature. An IS1 interferometric time series for the star Alpha Orionis is shown in Fig. 1. These data were taken on 8 September 1992 on a 13-m baseline. There are points in the time series when a cycle may have been incorrectly assigned, but by and large the phase seems properly connected.

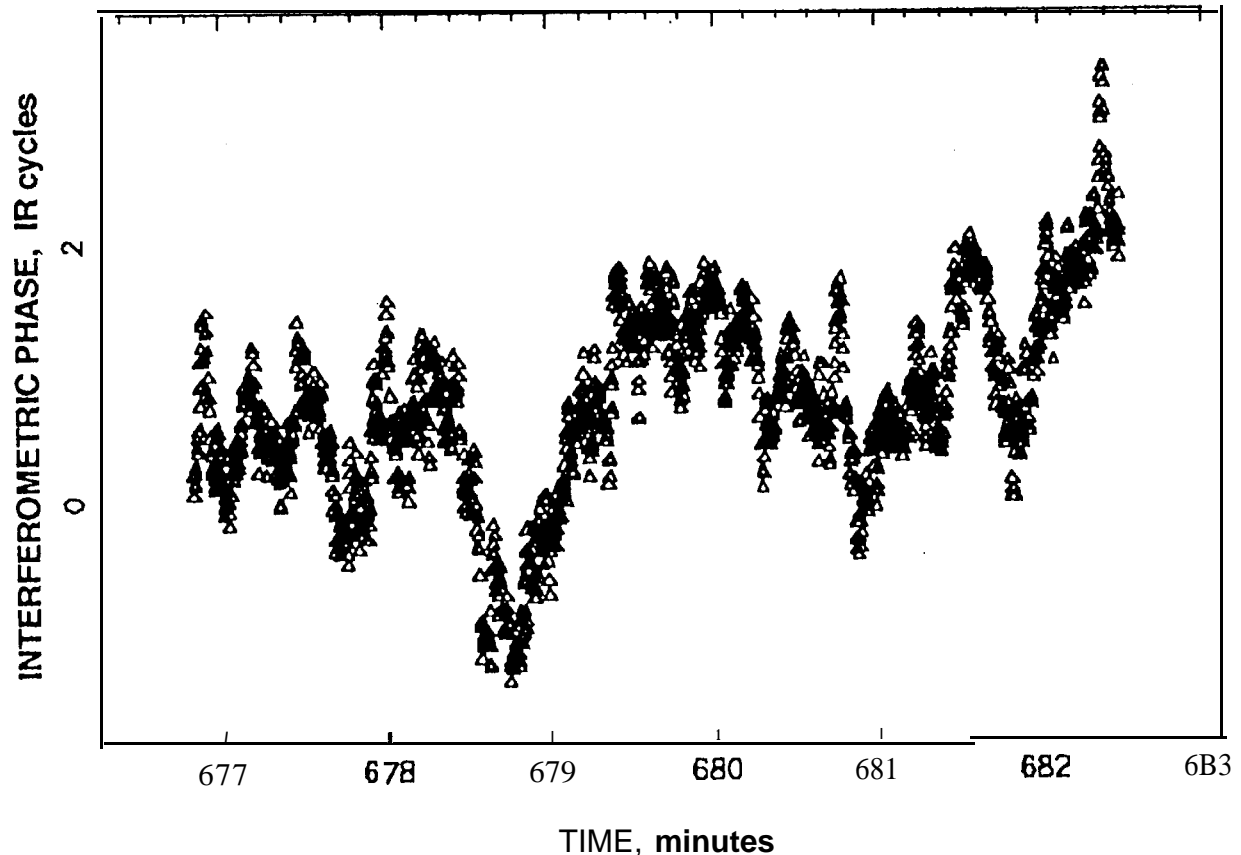


Fig.1: Infrared interferometric phase, in infrared ($11\mu\text{m}$) cycles, as a function of time for the star Alpha Orionis on 8 September 1992.

A general requirement on the sensitivity of astrometric devices is that the white (quantum or thermal) noise be low enough to allow integration times short compared to those characteristic of appreciable propagation media effects. For interferometric devices, both white noise and low-frequency peaked propagation noise contributions to the phase must be small enough to allow phase connection.^{3,4} Usually rms phase variations ≤ 0.1 cycles guarantee reliable phase connection. These qualitative statements are illustrated quantitatively in Fig. 2, which shows the point-to-point rms phase variation as a function of integration time, for the data of Fig. 1 and for Alpha Orionis data taken on 12 October 1989. Between the two epochs shown in Fig. 2, a number of sensitivity enhancements were made, including the installation of an improved heterodyne detector in one telescope of the 1S1. Low-frequency-peaked atmospheric effects increase as the integration interval increases. Quantum noise from the heterodyne detectors, on the other hand is white, or frequency independent, and should therefore average and produce smaller rms phase variations with increased integration time. The decreasing trend with increasing integration times until about 0.2 seconds is presumably due to quantum noise, while the increasing trend from 0.2 seconds on is associated with atmospheric refractivity fluctuations. The minimum rms phase fluctuation, i.e. the point at which the system noise and atmospheric trends cross, determines the optimal integration time. As can be seen from the figure, sensitivity upgrades improve performance by lowering the point-to-point fluctuation associated with the optimal integration time from about 0.2 cycles to about 0.13 cycles. If there were no rise in Fig. 2 due to atmospheric fluctuations, then integration times could be extended indefinitely and poor sensitivity could be tolerated. During nights of excellent seeing, for example on 10 October 1989, integration times of 1-second or more were used to connect phase.

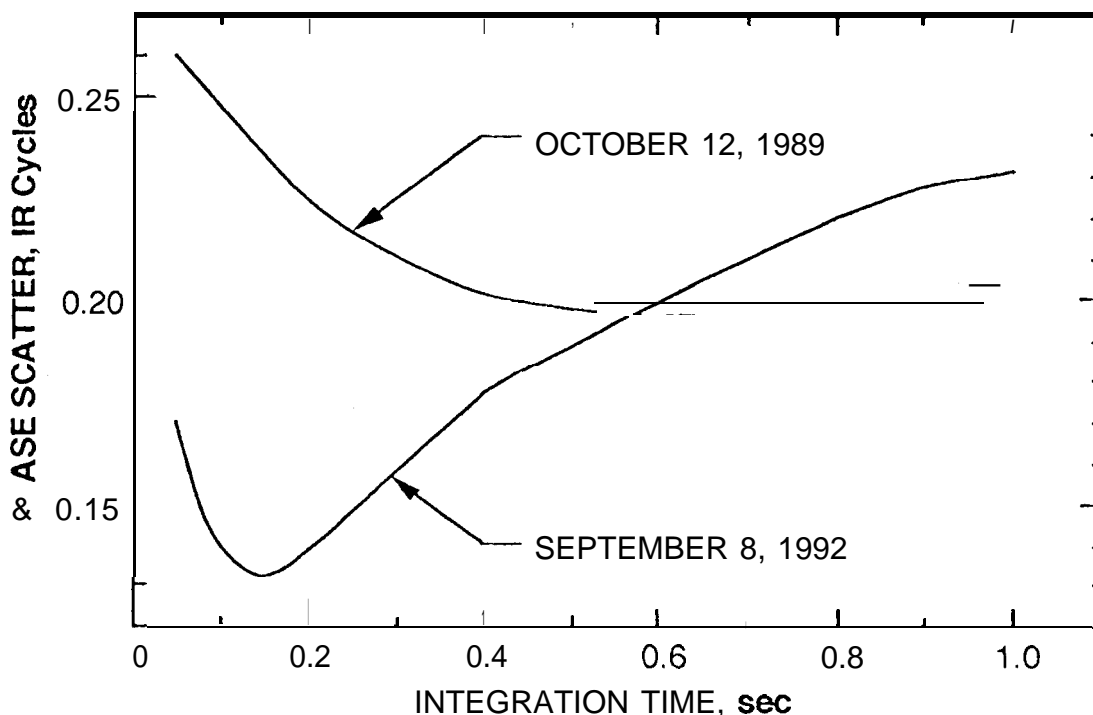


Fig. 2: The point-t-point rms phase scatter, in infrared cycles, as a function of integration time for the data of Fig. 1, and for Alpha Orionis data taken on 12 October 1989.

Fig. 2 thus illustrates the relationship between sensitivity and atmospheric fluctuations. Based on Fig. 2, "good seeing" will be defined from hereon as describing atmospheric phase fluctuations which are of the order of 0.1 infrared cycle ($\approx 11\text{pm}$) on 0.2-second time scales. Reliable phase connection requires slightly better sensitivity than that evidenced in Fig. 2 for typical Mt. Wilson observing conditions, for a bright star like Alpha Orionis. Future hardware upgrades, including installation of a new heterodyne detector in the other telescope of the 1S1, should improve the potential for phase connection, and therefore for infrared astrometry.

In addition to 1S1 sensitivity, systematic instrumental effects were studied by examining HeNe LDI path delay time series. They revealed resonances which may originate from the movement of the telescopes while tracking, or from resonances in the power supply. The resonances were at about 7 Hz, but sometimes multiple resonances between 1 and 10 Hz were found. The amplitudes of those resonances are such that they just barely contribute to infrared phase instability, but because they occur at frequencies which might cause additional problems with phase connection, we will attempt to identify and minimize them.

3. ATMOSPHERIC MODELING AND ERROR ANALYSIS

The discussion of atmospheric errors in this section assumes that phase connection problems will be solved by improved 1S1 sensitivity, as mentioned above. With reliable phase connection, the atmosphere still limits astrometric accuracy by causing path length changes which differ between the two telescopes of the 1S1. This section discusses the altitude dependence of the fluctuations as derived from model calculations, and the optimal use of HeNe LDI data to minimize atmospheric effects.

In Fig. 3, the Alpha Orionis data from 8 September 1992 are shown again, plotted with the telescope-differenced HeNe LDI path lengths, multiplied by 3 to demonstrate the correlation, which is about 0.6. That the factor of 3 applied to the HeNe LDI data yields fluctuations which more closely resemble those of the interferometric time series, suggests simple subtraction of the telescope-differenced HeNe LDI path delays from the interferometric delays is suboptimal.³ The time series in Fig. 3 prompted a model calculation to explore the optimal utilization of the HeNe LDI data in the asymmetric analysis, and to assess the resulting astrometric accuracy. A calculation of the expected level of correlation between HeNe LDI and interferometric path delays was performed using a modified Kolmogorov-Taylor formalism⁴, and implemented with the numerical techniques described by Bierman.⁵

The total interferometric path length due to non-zero tropospheric refractivity $\tau_{trop}(\theta, \phi, t)$ at elevation angle θ , azimuth ϕ relative to the orientation of the 1S1 trailers, and time t is given by

$$\tau_{trop}(\theta, \phi, t) = \tau_{atm}(\theta, \phi, t) + 2\tau_{HeNe}(t) \quad (1)$$

where $\tau_{atm}(\theta, \phi, t)$ is the contribution to the interferometric path delay from the differences in atmospheric refractivity along the electromagnetic paths from the observed object to each of the two telescopes of the 1S1, and $\tau_{HeNe}(t)$ is the ground-based, one-way, telescope-differenced HeNe LDI path delay due to non-zero refractivity. The HeNe LDI path lengths are defined to lie along the x-axis. The factor of two in eq. (1) accounts for the double traversal of the HeNe LDI path by the infrared interferometric signal: Once from the flat mirror to the parabola and once from the parabola through the cat's eye to the optics table in back of the flat mirror.²

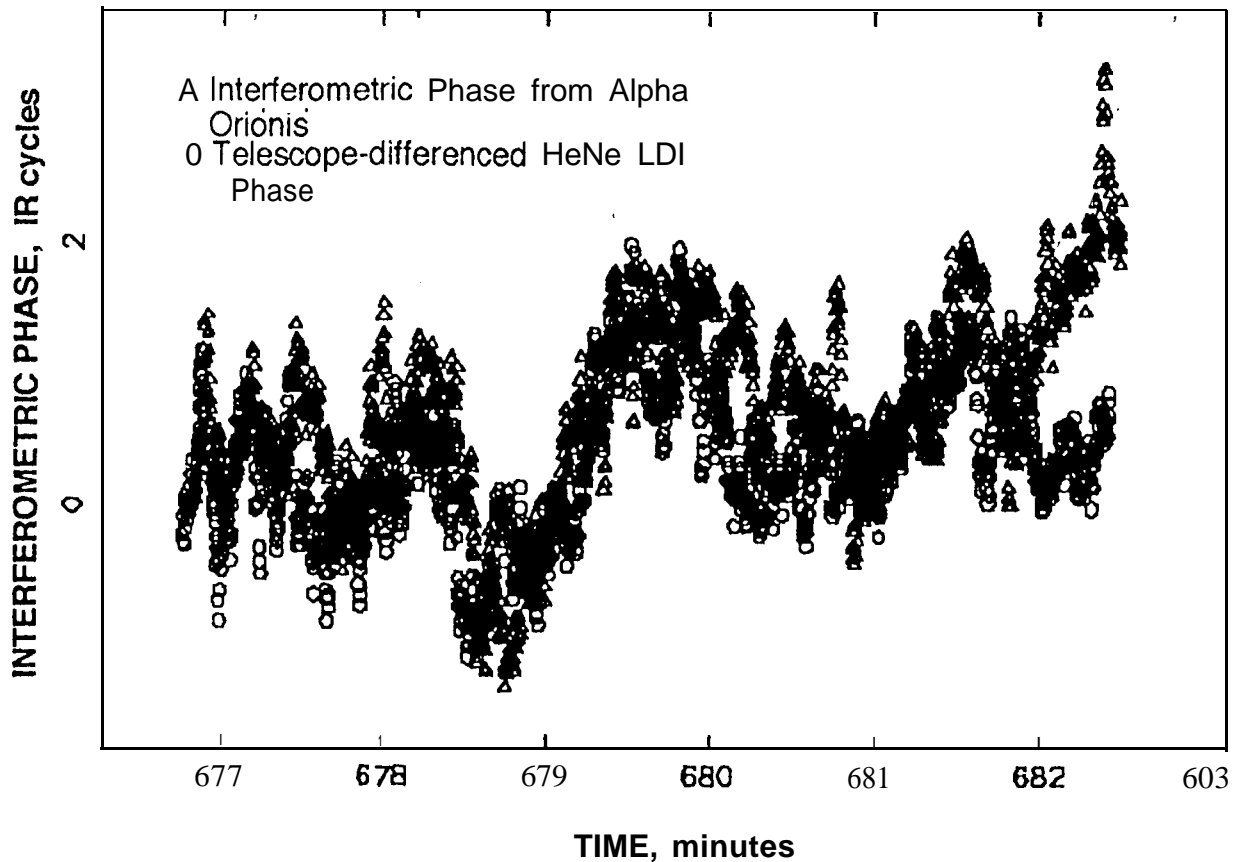


Fig. 3: The phase time series of Fig. 1 with the HeNe LDI phases, scaled to infrared cycles, difference between telescopes, and multiplied by 3.

The atmospheric and HeNe LDI path delay terms in eq. (1) are

$$\tau_{atm}(\theta, \phi, t) = \frac{1}{c \sin \theta} \int_0^h [\chi(\vec{r}_{2,atm}(\theta, \phi, z, t)) - \chi(\vec{r}_{1,atm}(\theta, \phi, z, t))] dz \quad (2)$$

$$\tau_{HeNe}(t) = \frac{1}{c} \int_0^l [\chi(\vec{r}_{2,HeNe}(x)) - \chi(\vec{r}_{1,HeNe}(x))] dx$$

where $\chi(\vec{r}_{i,atm})$ is the refractivity at the point denoted by the vector $\vec{r}_{i,atm}$ along the line of sight at height z above the i^{th} telescope. For the HeNe LDI delay, $\chi(\vec{r}_{i,HeNe}(x))$ is the refractivity at the vector position a distance x along the HeNe path for the i^{th} telescope. In eq. (2), h is the height of the turbulent atmosphere, l is the length of the HeNe LDI path, which is 5 meters, and c is the speed of light in vacuum. Using these expressions, the correlation ρ plotted in Fig. 4 is

$$\rho = \frac{\langle \tau_{trop} \tau_{HeNe} \rangle}{\sqrt{\langle \tau_{trop}^2 \rangle \langle \tau_{HeNe}^2 \rangle}} \quad (3)$$

where $\langle \rangle$ means ensemble average. The abscissa of Fig. 4 is h in eq. (2). The ensemble averages of refractivity were evaluated using Kolmogorov-Taylor structure functions, with a uniform structure

Do not type or paste anything outside this line. Type up to, but not beyond, the blue margin lines at left and right.

constant of $4 \times 10^{-7} m^{-1/3}$, a saturation scale of 10 meters, and a wind speed of 1 m/sec. These parameters were chosen to replicate the data of Fig. 3. The line-of-sight coordinates $(\theta, \phi) = (38^\circ, 71^\circ)$ were taken from the data of Fig. 3, and the horizontal line in Fig. 4 is p derived from the data of Fig. 3, assuming that a temporal average of p over a single scan is equal to an ensemble average over many scans (ergodicity). From Fig. 4, a 25-meter height is inferred for the turbulent atmosphere.

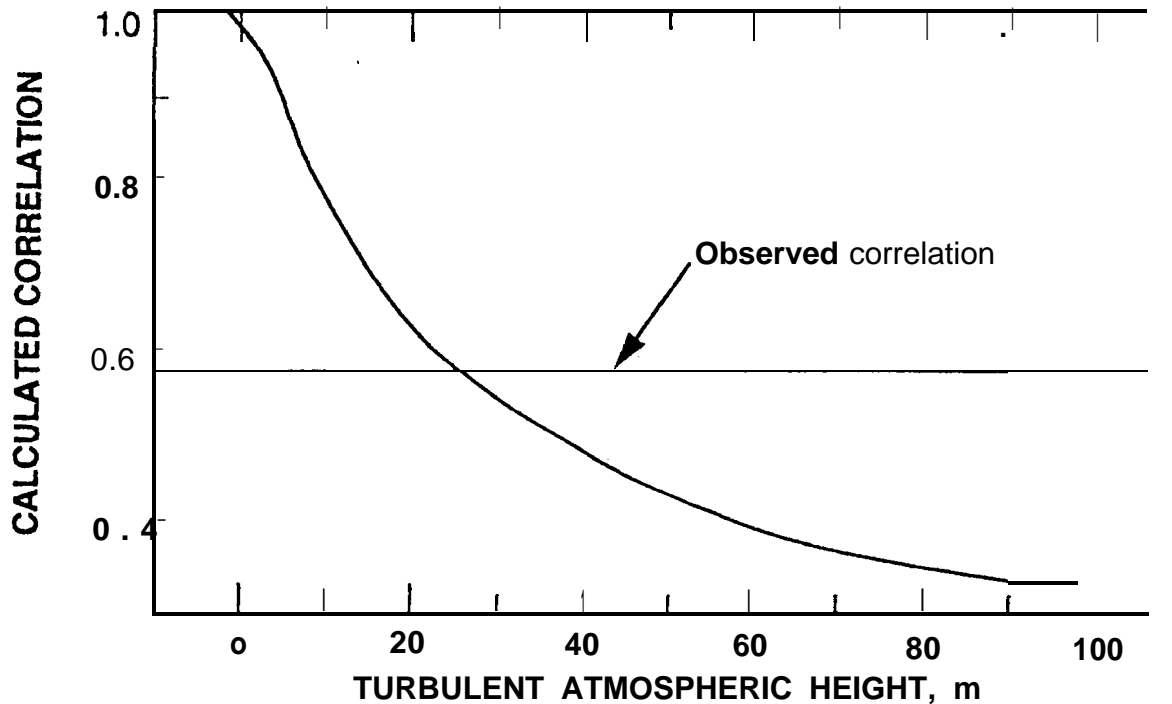


Fig. 4: The calculated correlation between the telescope-differenced HeNe LDI data and the interferometric data for the conditions of the data of Figs. 1 through 3. The horizontal line is the actual correlation from the data of Fig. 3

Fig. 4 suggests that the dominant atmospheric turbulence on nights of good seeing occurs within 25 meters of the ground. This inferred height has been determined assuming that there is a uniform structure constant to an altitude h in eq. (2). If an additional, weaker, higher-altitude turbulence component is postulated, then the correlation of Fig. 4 alone does not uniquely determine the altitude of the stronger, near-ground component. However, the ratio between the atmosphere-induced interferometric and HeNe LDI path delays would help to more uniquely constrain h . Calculations now in progress, which use this measured ratio, should produce a refined value of h , probably within a factor of 2 of that reported here.

The above atmospheric modeling can also be used to construct an optimal least-squares estimate for the interferometric delay at the middle of an observation interval, which is the fundamental quantity

This is the last line of the page. Do not type or paste below this line.

Do not type anything on this line.

of astrometric interest. The observed interferometric delay is modeled over a scan as

$$\tau_{int}(\theta, \phi, t) = \tau_0(t_0) + (t - t_0)\dot{\tau} + \tau_{trop}(\theta, \phi, t) \quad (4)$$

where $\tau_0(t_0)$ is the delay at the scan reference time t_0 , and the changes in θ and ϕ due to sidereal tracking during the scan have been ignored. The τ_0 delay includes offsets due to baseline and celestial source coordinates which differ from those used in the lobe rotator model of the 1S1 correlator. In eq. (4), $\dot{\tau}$ is a linear delay rate. The observed HeNe LDI delay is assumed to be given by eq. (2). An optimal estimate for τ_0 can be formed⁶, and its error standard deviation calculated using the covariance of τ_{trop} between all times t_i and t_j , which, suppressing the θ and ϕ arguments, is given by

$$\text{COV}(\tau_{trop}(t_i), \tau_{trop}(t_j)) = \langle \tau_{trop}(t_i)\tau_{trop}(t_j) \rangle - \langle \tau_{trop}(t_i) \rangle \langle \tau_{trop}(t_j) \rangle \quad (5)$$

The two ensemble averages in the second term on the right of eq. (5) are nearly zero for an interferometer with both telescopes at the same site. The covariance between the HeNe LDI delays, and between the interferometric and HeNe LDI delays must also be calculated. The above formalism^{4,6} can then be used to evaluate the ensemble averages which result after inserting expressions from eq. (2) into the first term on the right of eq. (5), and into the analogous equations including HeNe LDI delays. The resulting calculated, troposphere-limited, error standard deviations for angular astrometry are shown in Fig. 5.

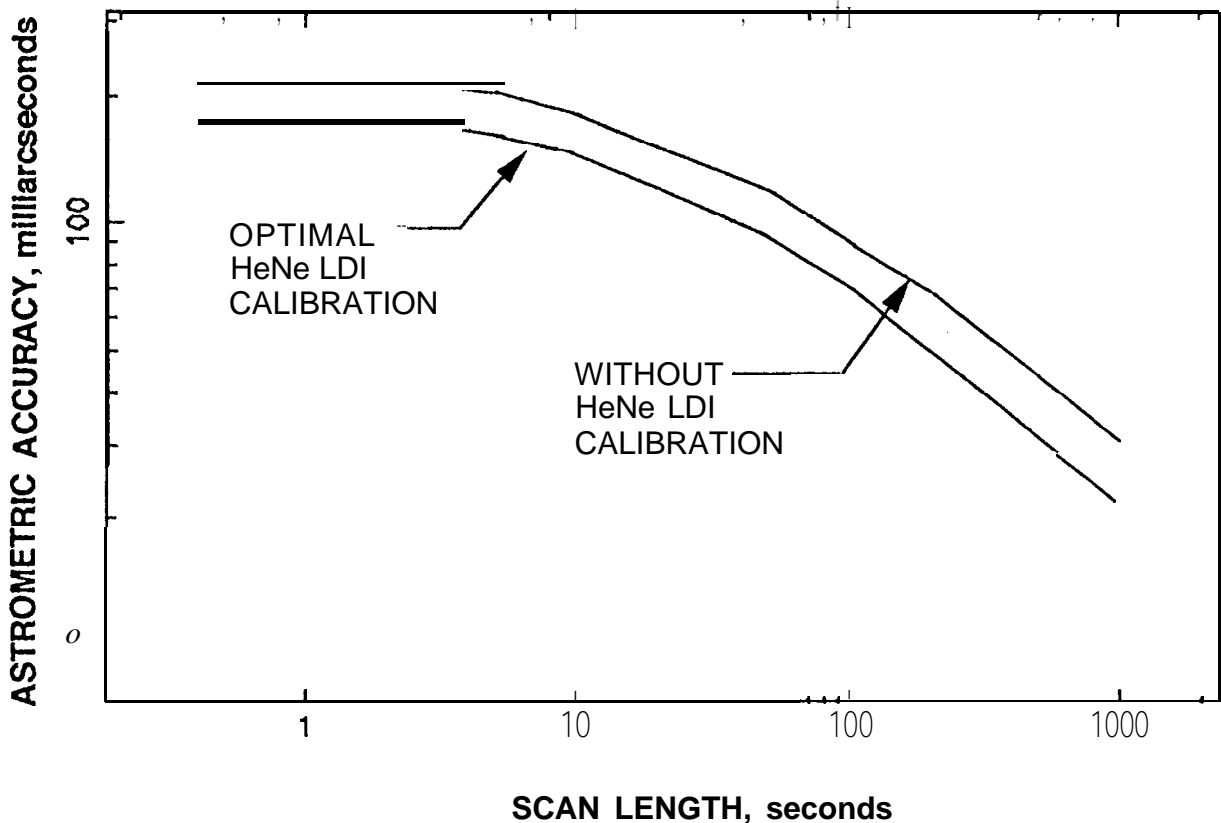


Fig. 5: The calculated astrometric accuracy, as a function of scan length, with and without optimal HeNe LDI calibration, for the conditions of Figs. 1 through 3.

The astrometric accuracy is c/B times the standard deviation for τ_0 in eq. (4), for a 13-m baseline length B , as a function of scan integration time. All turbulence parameters were the same as in the calculation of eq. (3), with the atmospheric height equal to 25 m. The upper curve shows the effect of the refractivity fluctuations in the absence of HeNe LDI calibration, and the lower curve shows the improvement if the current HeNe LDI calibrations are optimally used. For 1000-second scans, 20 mas accuracy seems attainable for interferometry with optimal HeNe LDI calibration. For azimuths along the HeNe LD1 path, the HeNe LDI-calibrated accuracy is improved by about 20%.

It should be noted that estimation procedures, which are calculationally simpler than the optimal procedure described above, may be used in actual data analysis; a negligible loss in astrometric accuracy may result. The formulation using eqs. 1-5 was presented to give insight into the turbulent atmospheric distance scales, the nature of ρ , and the reduction in astrometric error using HeNe LD1 calibration.

In addition to the optimal analysis of the HeNe LDI and interferometric path delays, the results of Fig. 4 suggest that local measurements of refractivity in the first 25 meters of the atmosphere may yield better than 20-mas astrometry, for observations when the HeNe LDI correlation is high. These local measurements could be meteorological or could consist of additional HeNe 1,1)1's which sample the vertical paths above the 1S1. It is very important to note that the above approaches which exploit the high correlation between the HeNe LDI and atmospheric path delays may have limited utility. On many nights in 1992 and 1993 observing seasons, with poorer seeing than that of 8 September 1992, HeNe LDI fluctuation levels not much different from those of Fig. 3 were observed, while the interferometric fluctuations were much larger than those of Fig. 3. Because the large fluctuations prevented reliable interferometric phase connection on those nights, the width of the power spectrum of the fringe amplitudes coming from the 1S1 correlator was used as the measure of the fluctuation level. That the interferometer signal was correlated with the HeNe LDI delays on nights of good seeing and much less so on nights of poorer seeing suggests the following picture characterizing the Mt. Wilson atmosphere: During relatively good seeing, the dominant atmospheric fluctuations are fairly low to the ground (within the first 25 meters) and optimal incorporation of HeNe LDI data and/or other ground-based calibration strategies may yield 20-mas or better infrared astrometry. During poorer seeing, substantial atmospheric fluctuations occur much higher than 25 meters above the 1S1 and neither HeNe LDI data nor ground-based calibration schemes will be of much help. In that case, laser guide star technology may prove useful. This hypothesis is consistent with the picture of the atmosphere in ref. 3, in which larger lateral saturation scales are attributed to nights of poorer seeing. The validity of this description of the atmosphere above Mt. Wilson and the ultimate astrometric accuracy of the 1S1 will be further explored with 1S1 data from the 1993 and 1994 observing seasons.

4. SUMMARY AND FUTURE DIRECTIONS

Instrumental and atmospheric effects currently limit infrared astrometry with 1S1. While instrumental system noise can prevent reliable phase connection, it has been shown that recent 1S1 upgrades have enabled a point-to-point phase scatter on 0.2-second time scales of about 0.13 infrared cycles for good seeing conditions. A factor of 2 improvement in the point-to-point phase scatter would greatly increase the reliability of interferometric phase connection.

Analysis and modeling of the 1S1 data suggest a two-component profile for the turbulent atmosphere above Mt. Wilson. For good seeing conditions, an approximate 25-meter turbulent atmospheric

height has been inferred, based only on the correlation between HeNe LDI and interferometric path length fluctuations, assuming a uniform structure constant. In the near future, this modeling will include the measured ratio between the rms interferometric and HeNe LDI path delays, thereby accounting for possible weaker, higher-altitude turbulence components. For poorer seeing conditions, the correlation is weaker suggesting that the turbulent atmosphere has substantial components above 25 meters. This modeling was also used to determine that the atmosphere-limited, single-source astrometric accuracy on an ISI 13-meter baseline during good seeing, with optimal HeNe LDI calibration, is about 20 mas for a 1000-second scan. Accuracy at this level would be approximately a factor of 4 better than previous infrared astrometric results.¹

Only single-source phase traces and atmospheric modeling have been used to infer the potential astrometric accuracy of the ISI. Multiple-source astrometry will require developing acquisition or analysis techniques to resolve cycle ambiguities between observations of multiple sources. Future astrometric improvements may include local monitoring of atmospheric effects to improve accuracy on nights of good seeing. Such monitoring could involve a combination of meteorological sensors and new HeNe LDI paths. In the more distant future, the development of an infrared, stellar reference frame will be pursued. A direct-detection (as opposed to heterodyne) system is being considered for the ISI on 5-year time scales. Direct detection would greatly increase the usable ISI bandwidth and sensitivity, enabling astrometry in a much wider variety of seeing conditions.

It should be noted that because of the apparent small lateral saturation scale during periods of good seeing, increases in baseline length will yield almost proportionate improvements in accuracy for sources which are not resolved. More importantly, atmosphere-induced errors for observations from the same session, or from different sessions, should be uncorrelated. By averaging results over many observations, astrometric accuracies of better than 10-mas should be possible.

5. ACKNOWLEDGMENTS

This work represents one phase of research carried out at the Jet Propulsion Laboratory, California Institute of Technology, under contract with the National Aeronautics and Space Administration. It was also supported by grants from the United States Office of the Chief of Naval Research (N00014-89-J-1583) and the National Science Foundation (AST-91 19317).

6. REFERENCES

- [1] E. C. Sutton, S. Subramanian, and C. H. Townes, *Astron. Astrophys.*, Vol. 110, p. 324, 1982.
- [2] M. Bester, W. C. Danchi, C. G. Degiacomi, and P. Bratt, paper 2200-26, this volume.
- [3] M. Bester, W. C. Danchi, C. G. Degiacomi, I. J. Greenhill, and C. H. Townes, *Ap. J.*, Vol. 392, p. 357, 1992.
- [4] R. N. Treuhaft, and G. E. Lanyi, *Rad. Sci.*, Vol 22, p. 251, 1987.
- [5] G. J. Bierman, Factorization Methods for Discrete Sequential Estimating, Academic Press, 1977.
- [6] W. C. Hamilton Statistics in Physical Science, Ronald Press, New York, 1964.
- [7] R. K. Tyson, Principles of Adaptive Optics, Academic Press, Inc., Boston, 1991

Treuhaft